Chemical Physics 531 (2020) 110653

Contents lists available at ScienceDirect

Chemical Physics

journal homepage: www.elsevier.com/locate/chemphys

A simple lattice Monte Carlo simulation to model interfacial and crowded water rearrangements

Ved Prakash Roy, Kevin J. Kubarych*

Department of Chemistry, University of Michigan, 930 N. University Avenue, Ann Arbor, MI 48109, USA

ABSTRACT

A finite, two-dimensional lattice model of liquid water captures the essential nearly four-coordinate hydrogen bonding network, while permitting a simple Metropolis Monte Carlo simulation in conditions ranging from crowded to dilute. This model examines excluded volume perturbations of hydrogen bond switching, avoiding complex topological and chemical heterogeneity of realistic interfaces. Retardation factors (relative to bulk) for switching agree with previous statistical models and atomistic molecular dynamics simulations of hydrated proteins. The model enables straightforward spatial mapping of retardation factors that are difficult to measure in atomistic simulations. The spatially-dependent retardation factors decrease exponentially from the interface. Simulating varying degrees of crowding, we do not find any cooperative, collective contributions anticipated from some recent spectroscopic observations suggesting correlated hydrogen bonding rearrangements of confined water. Longer-range cooperative interfacial influences may arise from complex chemical patterning of the surface, or to non-entropic influences such as multi-body interactions or altered hydrogen bond strengths.

1. Introduction

Understanding structural and dynamical fluctuations of water near hydrophobic interfaces poses challenges of practical and fundamental importance in chemistry, biology, and physics [1–5]. The hydrophobic effect can generally be understood as arising from the disruption of hydrogen bonding among water molecules upon addition of a solute [6–8]. The structural and thermodynamic consequences of solute hydration have been understood for many years [9,10], but there is considerably less consensus regarding the nature and degree of the solute's perturbation of water dynamics [2,11]. There are two interrelated issues that must be addressed in fully characterizing interfacial hydration dynamics. The first is the degree and nature of a single interface's influence over the motion of water molecules, as well as the spatial extent of this perturbation as a function of the distance from the interface. The second challenge is to understand how multiple interfaces modulate the dynamics of interstitial water molecules, and the degree to which there is, or is not, any collective, non-additive behavior.

An extensive interdisciplinary effort has been directed at this problem, combining spectroscopy, simulations and theoretical methods, but there are still open questions and contradictions [2,3,12,13]. A significant fraction of the experimental literature, and hence simulations, focus on biomacromolecular interfacial hydration for systems such as proteins [14–16], lipids [17,18], micelles [19,20] and nucleic acids [21]. Experiments typically make use of spectroscopic probes that may be intrinsic components of macromolecules, or covalently attached to specific sites. While the site-selective approach may have the advantage of enhancing signals arising from the interface, it is almost impossible to discern experimentally whether the observed dynamics results from the water alone or contains contributions from fluctuations of atoms or residues at the site of labeling. Alternatively, it is possible to use careful difference methods that isolate the interfacial contribution to steady-state Raman and THz spectra [22–29], even at lower solute concentrations. Some of these approaches depend on complex models to deconvolve the interfacial signal from that due to the bulk [30]. When relative concentrations of the macromolecular component are high, it becomes possible to use water's local vibrational modes to sense dynamics near an interface, but only under conditions corresponding to significant crowding [31]. Studies using small reverse micelles effectively bridge these two regimes: the water is automatically confined to the nanoscale vesicle, but studies of the water necessarily average over both interfacial and bulk-like water in micelles large enough to consist not entirely of interfacial water molecules [1,32,33]. Understanding how interfaces impart the slowdown of water dynamics is crucial for modeling the effect of crowding and understanding various biochemical process such as ligand binding to an enzyme, protein-protein interactions, and targeted drug delivery.

1.1. Summary of the extended jump model and interfacial perturbations

In the immediate vicinity of an interface, water hydrogen bond

* Corresponding author.
E-mail address: kubarych@umich.edu (K.J. Kubarych).

https://doi.org/10.1016/j.chemphys.2019.110653
Received 6 February 2019; Received in revised form 21 October 2019; Accepted 3 December 2019
Available online 10 December 2019
0301-0104/

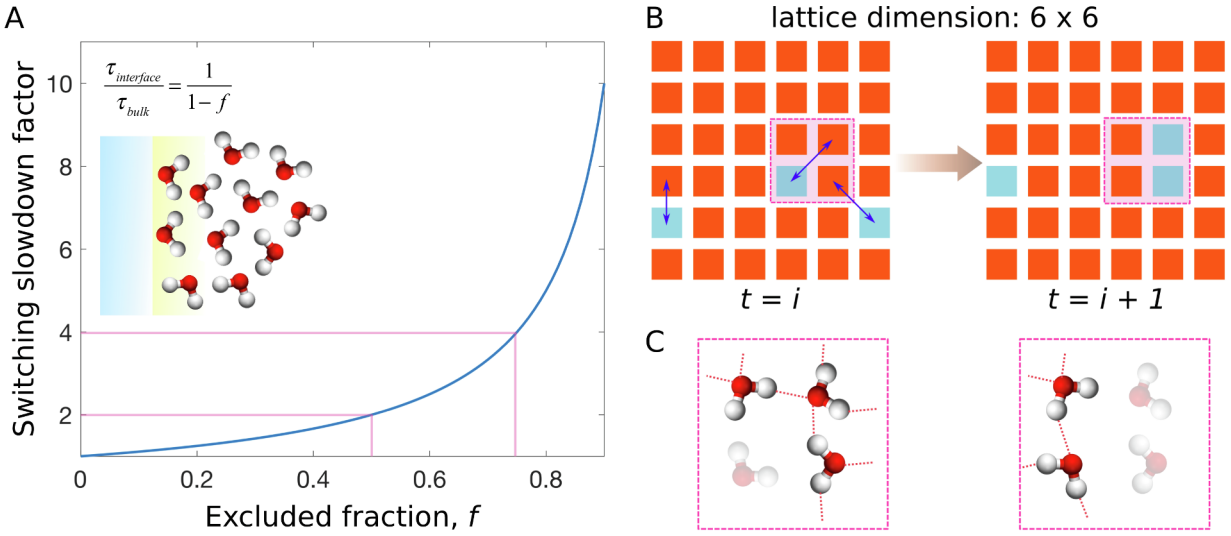

Fig. 1. (A) The predicted slowdown of hydrogen bond switching within the entropic, excluded volume model of Laage et al. shows a highly nonlinear dependence on the excluded water fraction. The cartoon highlights the local nature of this model, which would predict explicit perturbations for only those water molecules in the first solvation shell. This work aims to test whether there are any indirect, longer-range perturbations. (B) Schematic representation showing the implementation of a Monte Carlo simulation in a 6 × 6 lattice. Occupied sites are represented in orange while empty sites are shown in blue. Each filled lattice sites can form a maximum of 4 bonds with its immediate neighbor. An occupied site can swap positions with its neighboring vacant site along any of the eight directions. The Metropolis algorithm is implemented to determine whether a move is accepted or not. A move is taken only if the overall energetic cost of the swap is favorable, or if the Boltzmann factor is greater than a random number between 0 and 1. (C) Site switching dynamics in square lattices is analogous to the hydrogen bond switching event where bulk water molecules constantly exchange hydrogen bonding partners. A sub-selection of the lattice is shown to consist initially of 3 water molecules, and after rearrangement it only contains 2 water molecules with a different connectivity. Such fluctuations in the local coordination number of lattice sites mimics hydrogen bond switching events.

switching dynamics is perturbed due to the reduced fraction of available partners (f), which increases the free energy barrier for the extended jump mechanism, which is a three-body, termolecular elementary reaction [34,35]. Based on this purely entropic constraint, the retardation factor can be predicted to be two-fold near a planar interface, increasing nonlinearly with excluded water fraction (Fig. 1(A)). Within this model, to achieve an order-of-magnitude slowdown requires a 90% depletion of hydration water, which is limited to highly constrained geometries such as clefts, pockets, or grooves. Nevertheless, studies using dynamic fluorescence Stokes shift spectroscopy find evidence for extremely slow water, which would demand nearly full dehydration within the excluded volume picture [16,36–38].

One aspect of the excluded volume model apparent from Fig. 1(A) is the intrinsic locality of the perturbation. Although the water molecules directly in contact with the interface experience the full depletion of hydrogen bonding partners, the second hydration shell has the same number of neighboring water molecules as would be found in the bulk. Thus, the purely entropic slowdown can only apply to the first shell. The expectation is that the slowed first shell will somehow transmit its retardation to the second shell dynamically, but that coupling is mechanical rather than entropic. Significant experimental effort continues to be made to test the validity of the anticipated retardation of water dynamics at distances beyond the first hydration layer [39]. It is this aspect of the excluded volume contribution to crowding collectivity that we seek to assess with the present model.

The surface of any biological interface, such as a protein or membrane, consists of rugged topology and chemical heterogeneity. Although it is expected that concave curvature slows and convex curvature speeds up water dynamics [3,35,40,41], it is not clear to what extent the perturbation of dynamics extends outward from any arbitrary surface. Simulation studies of water dynamics near proteins and nucleic acids necessarily include structural and chemical heterogeneity of the interface, and the measured overall retardation factor may have contributions from a variety of influences. Hence, it may be important to understand how surface ruggedness contributes to the overall slowdown.

Remarkable progress in treating water with ever more sophistication, aided both by theoretical and computational advances, has led to the explicit representation of water polarization [42], many-body interactions [43], electron correlation [44] and nuclear quantum effects [45]. These new physical models are able to account for phenomena that are generally missing from the fixed-charge classical force fields popular in molecular dynamics simulations. It is certainly an important goal to simulate water accurately in biologically relevant systems using the most sophisticated level of theory. But, remarkably, many usual and unusual properties of water emerge from simulations using very simplistic models [46], such as the two-dimensional Mercedes-Benz [46–48], fixed three-point charge force fields (SPC, TIP3P) [49], and even single atom models [50].

Using a Metropolis Monte-Carlo simulation, we present a simple approach to model water's local connectivity and hydrogen bond (HB) switching dynamics in 2-D square lattices. We find that we can tune the model to give good agreement with structural (average coordination number or "degree") and dynamical properties (slowdown factors near an interface) compared to bulk water. In this work, we have also attempted to understand the switching dynamics at sites near an interface where surface topological heterogeneity is well characterized, and interactions can be eliminated. Our simple lattice model is poised to supplement the existing understanding of water dynamics near an extended interface. A key finding of our work is that the average switching correlation time falls off exponentially from the lattice boundary (i.e. the interface). Also, the slowdown in constrained systems can be modeled using a linear combination of individual interfaces, indicating that within this model there is no cooperative, non-additive behavior. We believe that in order to observe cooperative slowdown, a rugged surface heterogeneity may be essential in addition to taking into account longer ranged inter-particle interactions or modifications to hydrogen bond strengths.

2. Methods

2.1. Monte Carlo simulation of site switching on square lattices

Although Monte Carlo simulations are currently popular methods for sampling configurational ensembles, since the 1970s, Monte Carlo methods have been used to study relaxation [51] in cases where the mechanism is assumed to be a stochastic trajectory in equilibrium with a heat bath. In such models, barriers are treated as inputs to the simulation, and dynamical quantities such as time correlation functions can be computed. Early examples studied Ising models of 2D lattices of spins [52], and the equilibrium fluctuations of, for example, the magnetization could be analyzed as a function of temperature [51]. The main criterion to be satisfied in employing MC for dynamical phenomena is that the transitions between states obey detailed balance, which is a basic feature of the Metropolis algorithm for an equilibrium system [53]. Today this class of approaches to modeling activated processes in a time-domain manner is referred to as "kinetic Monte Carlo," [54] and recent work has shown that it is possible to determine real-time dynamical time scales from such simulations, rather than simply a non-dynamical Monte Carlo iteration step [55]. Essentially our model for water is a type of Ising model where sites can take on two states (bonded or unbonded), and the interaction energy is pairwise.

Empty (all zeros) 4 × 4, 6 × 6, 8 × 8, 10 × 10, 20 × 20 and 25 × 25 square lattices (arrays) are constructed. Each site in the lattice is occupied with particles (1 for particles and 0 for voids) with a filling probability of 0.9. Two neighboring particles are understood to form a bond if they share an edge. This 4-connectivity scheme and the 0.9 filling probability ensures that the average number of bonds for each particle in the lattice mimics the average hydrogen bond number in bulk water. Bulk water is expected to have an average coordination number of 3.6, considering 10% defects [56]. Rigid boundary conditions create an interface that can be considered hydrophobic. The average coordination number of sites at flat or curved interfaces will have reduced connectivity. Vacant sites in the lattice can make random moves along any of the 8 available directions in the square lattice. Since we maintain an occupation probability of 0.9, an occupied site can only be swapped with a vacant site. The Metropolis algorithm performs particle position switching based on an energetic criterion. A move is accepted if the Boltzmann factor ($e^{-\Delta E/RT}$) is greater than a uniform random number generated between 0 and 1. Simulations are performed for 50,000 iterations (time) and temperature is set at 298.15 K during the run. An energy of 1 kJ/mol is arbitrarily chosen as the switching energy barrier between occupied lattice sites. This barrier is consistent with a picosecond timescale hydrogen bond switching time, though it has been otherwise been chosen arbitrarily (see supplementary information S5). The total energetic cost for switching a pair is determined by summing over all the energy differences that results from a new configuration.

The coordination number of each site in the lattice as a function of simulation time is utilized to compute the bond correlation function $C(t)$ given by:

$$C_k(t) = \langle n_k(0) n_k(t) \rangle$$

where $n_k(t)$ is the number of hydrogen bonds at each site, k. The average time constant is computed by integrating the normalized (i.e. $C(t = 0) = 1$) correlation function for each site in the lattice. 40 trajectories with different starting configurations of the lattice were averaged to construct the correlation map.

Here, we implement a Monte Carlo simulation to investigate the effect of confinement on the site switching kinetics. The swapping of occupied sites with vacant ones captures the essence of hydrogen bond switching processes. In the bulk liquid, water molecules continually form and break hydrogen bonds, and a molecule completing a switch first extends its coordination with a neighboring partner thereby forming a three-body transition state. After a successful neighbor swap, the coordination number of the original partner becomes depleted by one, hence creating a vacancy. Fig. 1(B) shows how this fluctuation in the position of vacant and occupied sites has been implemented in a 2-D lattice. For comparison, Fig. 1(C) shows an analogous hydrogen bond switch between water molecules in a sub-lattice between two frames.

In our simulations we have used as a time variable the number of iterations performed in the Monte Carlo simulation run. A direct relationship with absolute time would require complete knowledge of the phase space being sampled by the simulation as routinely implemented by classical MD. Hence, instead of computing the absolute time scale for switching slowdown, we report the retardation factor relative to a reference bulk-like time constant (see Supplementary Information S2).

Although Monte Carlo simulations are not dynamical in the sense of yielding a trajectory, they are nevertheless quite useful for modeling stochastic barrier crossings. Using the Metropolis procedure to simulate barrier crossings effectively assumes the validity of transition state theory (i.e. being in equilibrium with a transition state) [57]. Since the excluded volume arguments of Laage et al. are based on this assumption, we feel it is justified to use in this approach. Because the excluded volume picture is essentially due to the interfacial modulation of the entropic barrier to H-bond switching, it would seem that a Monte Carlo approach could highlight or even isolate that aspect. Although our 1 kJ/mol barrier is arbitrary, it is close to what would be expected for a picosecond timescale process. Nevertheless, within the Metropolis procedure, changing the barrier has the same effect as changing the temperature, or changing the time scale. Since we never extract any absolute time scales, and analyze only relative correlation function decays, the barrier value is largely inconsequential for determining the spatial dependence of the hydrogen bond switching kinetics.

3. Results and discussion

3.1. Spanning hydrogen bond network in bulk water

Before performing any dynamical analysis using Monte Carlo simulations, we first characterize the structural aspects of the model. Although it is common to analyze real-space atomistic structure using metrics such as radial distribution functions, in a lattice model, another useful measure of structure is the connectedness of the bonding network. Structurally, each point on the lattice represents a water molecule, which is itself a node in the network. Every occupied lattice site can form a maximum of four connections with its neighbors, which coincides with the typical maximum of 4 hydrogen bonds (2 donor and 2 acceptor) in water [44].

The extended network of hydrogen bonds of water is thought to play an important role in the functioning of macromolecules, particularly in crowded environments. At very low hydration, the extended network of hydrogen bonds can be broken significantly, giving rise to small patches of water clusters consisting of only a few molecules. Winter and coworkers [58] have previously shown that water clusters undergo a percolation transition at the surface of globular proteins in extremely low hydration environments. The structured water molecules in protein powders have also been shown to act as an entropic reservoir for the onset of native functioning of biomolecules [59].

Fig. 2 shows the largest cluster size in finite square lattices with varying occupancy probabilities of the sites. A cluster is defined as any collection of occupied sites where a given site can be reached from any other site in that cluster, provided they are connected by a shared side. Having multiple disjointed clusters results in the formation of small islands of fully connected paths. The "largest cluster" refers to the cluster with maximum number of occupied sites among all the clusters for a given configuration. The abscissa in Fig. 2 has been normalized by the total number of lattice sites (N^2). Occupancy probabilities from 0.3 to 1.0 were generated for lattices of size 25 × 25, 30 × 30, 40 × 40, 50 × 50, 60 × 60 and 70 × 70.

It is clear that the onset of the percolation transition starts around a

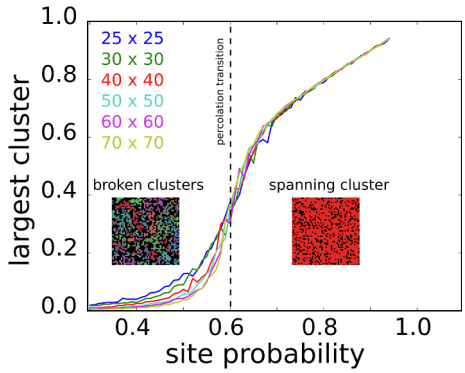

Fig. 2. Formation of spanning (completely connected) clusters in square lattices via a percolation transition with varying site occupation probability. Lattice sizes from 25 × 25 to 70 × 70 have been considered where formation of spanning clusters occurs at roughly the same transition probability of 0.6. At low occupation probabilities, patches of connected clusters emerge (bottom left inset) which coalesce to form one giant cluster after the percolation transition (bottom right inset). Considering 4-neighbor connectivity, this transition probability corresponds to an average degree (i.e. coordination number) of ~2.4 in bulk water.

probability of 0.5. Before the percolation transition, the lattice sites show patches of small clusters as represented in the inset of Fig. 2 on the bottom left. The percolation transition occurs at the inflection point at $p \sim 0.6$ (average degree ~ 2.4), and is independent of the lattice dimensions, a well-known result from percolation theory for infinite lattices [60–62]. The transition curve does appear to become steeper with increasing lattice sizes, implying that it is easier to form large clusters at the same probability in smaller square grids than in large grids. Such finite size effects are notable because rigorous theoretical values for the percolation transition are derived from infinite lattices. Beyond percolation ($p > \sim 0.7$), it is apparent that most of the sites in the lattice form a giant cluster. In this regime, the largest cluster size scales linearly with occupancy probability. Previously, Winter et al. [63] have shown that the onset of the percolation transition in liquid water occurs around the same coordination number (degree of 2.0–2.3) as observed with the simplistic square lattice model. The spanning water network on protein surfaces undergoes a 2-D percolation transition, which is also consistent with this lattice model [64].

3.2. Linear scaling of average coordination number with occupation probability

In previous sections, we established that the percolation threshold in liquid water corresponds to the threshold obtained using a square lattice model. Before interpreting any dynamical observables from our simulation, it is essential to characterize the local site connectivity in the lattice relative to that of bulk water. We find a quasi-linear trend in the average coordination number for sites with varying occupation probability in square lattices as shown in Fig. 3(A). Lattice sizes of 4 × 4, 10 × 10, 20 × 20, 50 × 50, 100 × 100, 200 × 200 and 400 × 400 have also been compared. For the extremely small lattice size of 4 × 4, where the perimeter to area ratio is 1, we observe a 27% decrease in the average coordination number compared to bulk coordination number of 3.6 at 0.9 site probability as shown in Fig. 3(B). A modest percolation threshold corresponding to an average degree of ~2.4 is also shown in the plot. Although, for small lattice dimensions, the average degree may appear to be smaller, we find that even at this bond connectivity only one giant cluster emerges. For all the lattice sizes, the average degree of sites studied in this work is well above the percolation threshold. In other words, we do not anticipate any crowding dynamical transition to be due to a percolation transition. Fig. 3(B) also indicates that with increasing lattice size the average

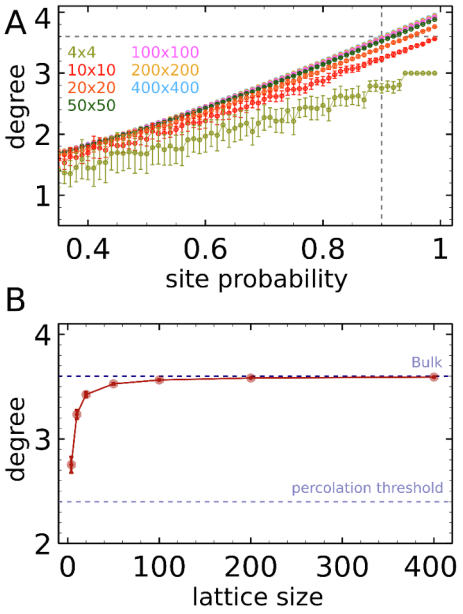

Fig. 3. (A) Average coordination number (i.e. "degree") calculated for different lattice sizes from 4 × 4 to 400 × 400 with varying occupation probability. A 4-neighbor connectivity is considered for calculating the coordination number of each occupied site. A clear linear trend emerges at large occupation probabilities. For Monte Carlo simulations, an occupation probability of 0.9 was used to ensure that the average coordination number remains ~3.6 (dashed line) mimicking bulk water's coordination. Each data point is the average of over 20 different random configurations and error bars represent one standard deviation from the mean. (B) Average coordination numbers in the different lattice sizes shown in (A) at the specific occupation probability of 0.9. The average degree converges to a value of ~3.6 with increasing lattice size, approaching the coordination number of bulk water.

connectivity converges to the bulk water coordination number of 3.6. In this work we have used square lattices with constant occupation probability of 0.9 to mimic hydrogen bond switching dynamics in a well-understood Ising-like model. In addition, systematic variations in lattice dimensions allows us to mimic the conditions of crowding.

3.3. Spatial extent of perturbation using square lattices

Protein interfaces present a diversity of chemical interactions. Laage et al. have previously reported that such heterogeneity does not have significant impact on the average retardation factor of hydrogen bond jumps near different protein residues [35]. Overall, a retardation factor of 2 should be expected right next to extended protein interfaces. The role of topology, however, is more pronounced, where clefts can induce much more dramatic jump retardation factors [40].

The swapping of empty and occupied sites in square lattices, implemented using Metropolis Monte Carlo, models hydrogen bond switching events. A filled site in the lattice represents water molecules whereas vacant sites represent an unfavorable hydrogen bonding partner (either donor or acceptor). Our MC simulation enables us to delineate contributions to dynamics arising from simple interfaces consisting of only flat sides and corners, though future work will consider more complex topology. The occupied sites at the interface have reduced coordination numbers since no periodic boundary is used. Small lattice sizes (4 × 4 or 6 × 6) represent higher degrees of crowding due their high perimeter-to-area ratio, while larger lattices (≥15 × 15) should be comparable to dilute, bulk-like environments.

We take as the bulk-like timescale that which is obtained from the fastest average time constant in the 30 × 30 lattice. Fig. 4(A–C) shows the retardation factor maps obtained by measuring average correlation times for switching vacant sites relative to bulk in 6 × 6, 15 × 15 and

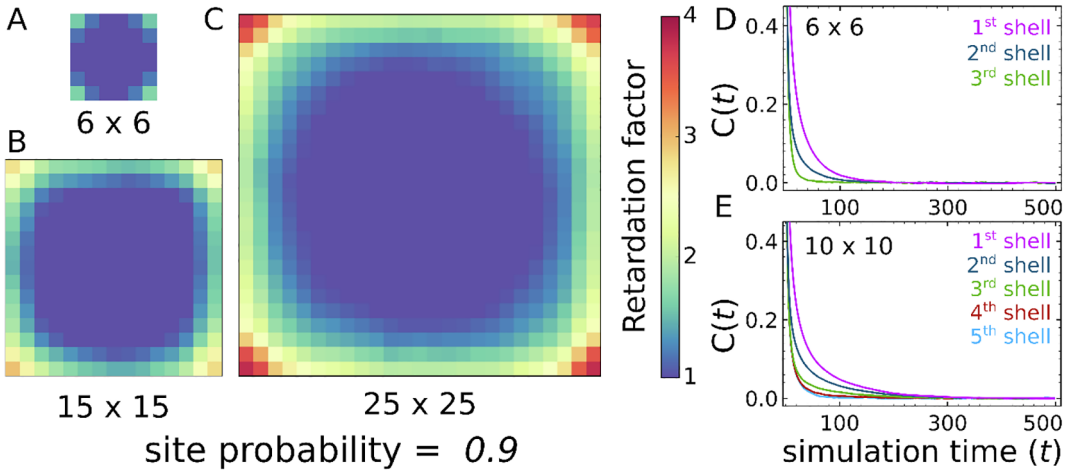

Fig. 4. (A) Retardation factor maps showing site switching dynamics in the 6x6 lattice with a filling probability of 0.9. Individual pixels represent retardation factors relative to the bulk water dynamics timescale obtained using a 30 × 30 lattice size (see Supplementary Information for fitting details). Simulations were performed via switching occupied and filled sites based on the Metropolis-Hastings algorithm. Average bond correlation times were obtained by integrating each correlation function up to 500 simulation iterations. Differences in the dynamics can be seen between the first and second shells. A retardation factor of 1 corresponds to a bulk-like timescale whereas larger values represent longer correlation times. (B, C) Retardation factor maps for 15 × 15 and 25 × 25 lattices, respectively. The observed retardation factor of 2 near flat interfaces is a direct manifestation of excluded volume effect. Enhanced retardation is also observed for sites near the corners consistent with a reduced fraction of available partners relative to the bulk. (D) Normalized (i.e. C(t = 0) = 1) correlation functions (shown up to 0.4 y-axis for clarity) in the 6x6 lattice indicate the maximum retardation for the first shell (closest to the interface), followed by the second and third shells. (E) Normalized correlation functions for first to fifth shells in the 10 × 10 lattice. Correlation decay times converge for the fourth and fifth shells confirming that the maximum perturbation length scale is roughly the third shell.

20 × 20 size lattices, respectively. A value of 1 represents bulk-like dynamics while larger values represent longer average correlation times. In this work we find that for lattice sizes that can accommodate more than two shells, the extent of the dynamical perturbation propagates, at most, to the third shell. Fig. 4(D) and (E) show calculated correlation decays for site switching dynamics in 6x6 and 10 × 10 lattices, respectively. The 6 × 6 lattice (Fig. 4(D)) exhibits shell-dependent time correlation functions. The slowest average correlation time is observed for the first shell, followed by the second and third shells. To determine the length scale on which dynamical perturbations propagate from the interface, we focus our attention on the larger 10 × 10 lattice (Fig. 4(E)). A 10 × 10 lattice provides the best chance for observing any additional contributions to the slowdown arising from potential cooperativity. This 10 × 10 lattice is the only size that can accommodate more than three shells while also maintaining a significantly high degree of crowding. As expected, time correlation functions for the first shell have the largest time constants (i.e. are slowest to decay) followed by the subsequent shells. The correlation times appear to converge around the third shell.

Our simulations show additional slowdown in cleft like geometries near the corners of the square lattice, as is particularly evident in Fig. 4(C). This finding is in accord with the predictions from the excluded volume fraction [34] as well as calculated compressibility studies [65] of water near an armchair carbon nanotube interface which concluded that a concave geometry is more hydrophobic than a convex geometry. The 4-fold slowdown agrees quantitatively with the $(1/[1-f]$, where $f = 0.75)$ prediction by Laage et al. Apart from entropic constraints imparted by an interface, Patel et al. have shown that patterned patches of hydrophilic sites influence water affinity [65]. NMR experiments measuring water diffusivity in different proteins exhibiting varying levels of surface topology have also found similar influences of curvature over hydrophobic interactions [66]. Enthalpic constraints imparted on water by different chemical patterns only influence molecules in the immediate vicinity of such interactions, whereas topology and patterning can be more delocalized [67]. In our lattice Monte Carlo simulations, we do not observe any additional retardation in correlation times near a flat interface, particularly in the smallest lattice dimensions.

3.4. Additive bond dynamics in constrained environments

Before discussing the non-additive switching dynamics, it is necessary to highlight some fundamental limitations of the present model and analytical approach. This simulation is governed by pairwise interactions and the main quantity analyzed is the time correlation function of site occupation, therefore our model is limited in its ability to capture larger scale collective dynamics [68,69]. This limitation is inherent to the design of the study, since a central aim is to determine to what extent the entropic excluded volume effect can also influence collective hydrogen bond rearrangements.

Since reducing the size of the lattice effectively increases the degree of crowding, we had anticipated that the constrained geometry would show non-additive slowdown in dynamics due to collective switching dynamics. As the perimeter-to-area ratio increases in smaller lattices, however, we see a reduction in the overall average bond correlation time as shown in Fig. 5. This effect is simply based on the differences in time required to sample the available configurations, which is a finite-size effect common in Monte Carlo simulations. For lattices of smaller dimensions, fewer iterations are needed to completely sample the available configurations while larger lattices will require longer time to sample the entire configuration space. We find a non-linear dependence in the overall timescale for site switching along the lattice axis. It is therefore of interest to explore any possibility of non-additive behavior when interfaces come close together. We take the largest lattice dimension (30 × 30, black curve in Fig. 5) to obtain distance-dependent dynamics in what we assume to be the absence of crowding.

The curves are fitted with two exponential functions with a constant offset, one from index 0 to 15 and the other from index 15 to 29. The constant offset parameter accounts for overall scaling of the average correlation time due to the finite size of the square geometry. Parameters of the fit are tabulated in Table 1 which are obtained using points taken along the lattice axis passing through the center.

The fit parameters obtained for the uncrowded case are then used to fit rest of the decay constant data from 4 × 4 to 25 × 25 lattices. We use the same sum of functions $[f_1(x) + f_2(N - x)]$ to fit the smaller lattices; fixing the decay constant (τ) and exponential amplitude (a) enables a direct test of the additivity in dynamics. Since the end index

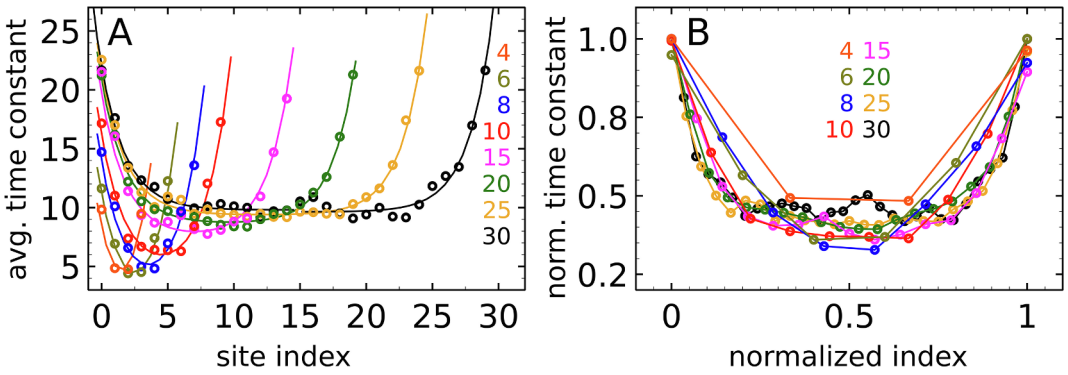

Fig. 5. (A) Average bond correlation time constants for lattices of different sizes along an axis passing through its center. Time correlation values along the x and y axes have been averaged to maximize statistical significance. The maximum slowdown is observed for sites in the first shell; the slowdown decays exponentially with shell index. Notice that due to the finite size effect, a speedup in the overall decay times for smaller lattice dimensions is seen. This speedup is not physical and is an artefact of Monte Carlo simulations that is removed by comparing relative time scales for decay. (B) A site-index (x-axis) and maximum decay rate (y-axis) normalized plot for data in (A) shows a size dependence that appears to be stretched for smaller lattice dimensions which could be interpreted as cooperativity. Instead, all of the size dependences are fit with the same exponential damping factor (shown Table 1).

Table 1
Parameters obtained for the exponential fit for average correlation times versus site index along the center axis in the 30x30 lattice as shown in Fig. 5.

Site index	Fitting function	Fit parameters		
		a	τ	c
0–15	$f_1(x) = ae^{-x/\tau} + c$	12.21	1.87	9.80
15–29	$f_2(x) = ae^{-(29-x)/\tau} + c$	12.32	1.82	9.63

(N) for different lattice dimensions vary, it is set to the size of the lattice that is to be fitted. This approach leaves the offset parameter, c of the fitting function as the only adjustable term. Fig. 5(A) also shows fits for the curves using solid lines. We find that all other lattice sizes can be fitted using a sum of fitting functions, which indicates a lack of any non-additive dynamics arising solely due to crowding.

In Fig. 4(C), due to increased hydrophobicity and a reduction in the availability of favorable neighbors (up to 75%), there is additional slowdown at the corners. Based on the observed trends in the time correlation map, we can conclude that flat interfaces are ineffective in imparting any non-additive slowdown in the hydrogen bond switching dynamics within the thermodynamic model used here. Additional slowdown in dynamics near sharp concave curvatures (i.e. at the corners of the lattice) hints at the idea that a rugged topology may be capable of inducing non-additive contributions. This analysis lacks explicit crowding-induced changes of the interactions between the surface and the water (eg. due to changes in the local dielectric), as is the precise goal here to eliminate this kind of detail, but these effects can certainly be expected to contribute to hydrogen bond switching perturbations.

4. Conclusion

A simple Monte Carlo simulation with square lattices captures the essential connectivity of hydrogen bond networks and the switching dynamics in liquid water. The main goal of analyzing such a model is to determine the spatial extent of the excluded volume perturbation of hydrogen bond dynamics in the complete absence of any interactions or complex surface topology, which is inevitable in atomistic molecular dynamics simulations. This simple model explicitly excludes any contribution to dynamics from fluctuations of the solvated biomacromolecules, which may confound atomistic MD simulations. Our approach relies on calculating hydrogen bond time correlation functions using a straightforward site swapping Metropolis method. Although our method cannot capture the orientational dynamics explicitly, the hydrogen bond switching inherently encodes the rotating water during the switching window.

By making the correspondence with the well-characterized phenomenon of percolation on 2D graphs, where there is a rigorous threshold at an occupation probability of ~0.6, we find that the connectivity in liquid water is above the percolation threshold given that accurate hydrogen bonding degree distributions require an occupation probability of 0.9. Our method also accurately describes the retardation factor for hydrogen bond switching due to an interface, which has previously been estimated using statistical mechanics and atomistic molecular dynamics simulations. The retardation factor maps for different size lattices show that the dynamical perturbation extends, at most, to the third hydration shell. Dynamical perturbation beyond this distance, which has experimental support, likely results from a mechanism not captured in the present model, or, more generally, one that is separate from the entropic excluded volume origin. The spatial dependence of the retardation factors appears to be size dependent, but we are able to reproduce results for all of the lattice sizes using only the ~2 site exponential decay found in the largest lattice. This finding is clear evidence for a lack of cooperative, non-additive behavior, and indicates that collective hydration dynamics associated with the complex coordinated rearrangements of water molecules are not captured with this model. Since our model captures quantitively the excluded volume prediction for the retardation factor in the corner regions of the lattice, the results suggest that controlled reintroduction of surface topological complexity can be used to test the origin of possible collective hydration dynamics. Multi-body interactions do contribute to non-entropic terms and are more pronounced right next to an extended interface. Many-body effects have been pioneered by Paesani et al. and have been found to be important in aspects of bulk and interfacial water, particularly regarding the computation of spectroscopic observables [70–73]. Since the hypothesis in this work is to capture contributions to the slowdown arising purely due to propagation of disorder by an interface, quantifying the site jump correlation as a function of crowding provides the best way to capture contributions to slowdown independent of surface heterogeneity. Although some recent spectroscopic observations suggest highly correlated hydrogen bonding rearrangements of confined water caused by the influence of multiple macromolecular interfaces, our results suggest that those perturbations are intrinsically dynamic, lacking an entropic contribution to the free energy landscape change.

Declaration of Competing Interest

The authors declare that they have no known competing financial

interests or personal relationships that could have appeared to influence the work reported in this paper.

Acknowledgement

This work was supported by the National Science Foundation (CHE-1565795).

Appendix A. Supplementary data

Supplementary data to this article can be found online at https://doi.org/10.1016/j.chemphys.2019.110653.

References

[1] M.D. Fayer, Dynamics of water interacting with interfaces, molecules, and ions, Acc. Chem. Res. 45 (2012) 3–14.
[2] W. Thompson, Perspective: dynamics of confined liquids, J. Chem. Phys. 149 (2018) 170901.
[3] D. Laage, T. Elsaesser, J.T. Hynes, Water dynamics in the hydration shells of biomolecules, Chem. Rev. 117 (2017) 10694–10725.
[4] B. Bagchi, Water dynamics in the hydration layer around proteins and micelles, Chem. Rev. 105 (2005) 3197–3219.
[5] J.N. Dahanayake, K.R. Mitchell-Koch, Entropy connects water structure and dynamics in protein hydration layer, Phys. Chem. Chem. Phys. 20 (2018) 14765–14777.
[6] K. Lum, D. Chandler, J.D. Weeks, Hydrophobicity at small and large length scales, J. Phys. Chem. B 103 (1999) 4570–4577.
[7] M.B. Hillyer, B.C. Gibb, Molecular shape and the hydrophobic effect, Annu. Rev. Phys. Chem. 67 (2016) 307–329.
[8] J.T. Titantah, M. Karttunen, Hydrophobicity: effect of density and order on water's rotational slowing down, Soft Matter 11 (2015) 7977–7985.
[9] T.V. Chalikian, Structural thermodynamics of hydration, J. Phys. Chem. B 105 (2001) 12566–12578.
[10] X.G. Wu, W.J. Lu, L.M. Streacker, H.S. Ashbaugh, D. Ben-Amotz, Temperature-dependent hydrophobic crossover length scale and water tetrahedral order, J. Phys. Chem. Lett. 9 (2018) 1012–1017.
[11] B.J. Berne, J.D. Weeks, R.H. Zhou, Dewetting and hydrophobic interaction in physical and biological systems, Annu. Rev. Phys. Chem. 60 (2009) 85–103.
[12] K.J. Kubarych, V.P. Roy, K.R. Daley, Interfacial water dynamics, in: K. Wandelt (Ed.), Encyclopedia of Interfacial Chemistry Elsevier 2018, pp. 443–461.
[13] C. Päslack, L.V. Schäfer, M. Heyden, Atomistic characterization of collective protein–water–membrane dynamics, Phys. Chem. Chem. Phys. 21 (2019) 15958–15965.
[14] J.T. King, E.J. Arthur, C.L. Brooks, K.J. Kubarych, Site-specific hydration dynamics of globular proteins and the role of constrained water in solvent exchange with amphiphilic cosolvents, J. Phys. Chem. B 116 (2012) 5604–5611.
[15] J. Yang, Y.F. Wang, L.J. Wang, D.P. Zhong, Mapping hydration dynamics around a beta-barrel protein, J. Am. Chem. Soc. 139 (2017) 4399–4408.
[16] L.Y. Zhang, L.J. Wang, Y.T. Kao, W.H. Qiu, Y. Yang, O. Okobiah, D.P. Zhong, Mapping hydration dynamics around a protein surface, Proc. Natl. Acad. Sci. U. S. A. 104 (2007) 18461–18466.
[17] G. Folpini, T. Siebert, M. Woerner, S. Abel, D. Laage, T. Elsaesser, Water librations in the hydration shell of phospholipids, J. Phys. Chem. Lett. 8 (2017) 4492–4497.
[18] A. Kundu, B. Blasiak, J.H. Lim, K. Kwak, M. Cho, Water hydrogen-bonding network structure and dynamics at phospholipid multibilayer surface: femtosecond mid-IR pump-probe spectroscopy, J. Phys. Chem. Lett. 7 (2016) 741–745.
[19] I.R. Piletic, H.S. Tan, M.D. Fayer, Dynamics of nanoscopic water: vibrational echo and infrared pump-probe studies of reverse micelles, J. Phys. Chem. B 109 (2005) 21273–21284.
[20] V.P. Roy, K.J. Kubarych, Interfacial hydration dynamics in cationic micelles using 2D-IR and NMR, J. Phys. Chem. B 121 (2017) 9621–9630.
[21] K. Kuchuk, U. Sivan, Hydration structure of a single DNA molecule revealed by frequency-modulation atomic force microscopy, Nano Lett. 18 (2018) 2733–2737.
[22] J.G. Davis, K.P. Gierszal, P. Wang, D. Ben-Amotz, Water structural transformation at molecular hydrophobic interfaces, Nature 491 (2012) 582–585.
[23] J.G. Davis, B.M. Rankin, K.P. Gierszal, D. Ben-Amotz, On the cooperative formation of non-hydrogen-bonded water at molecular hydrophobic interfaces, Nat. Chem. 5 (2013) 796–802.
[24] P.N. Perera, B. Browder, D. Ben-Amotz, Perturbations of water by alkali halide ions measured using multivariate raman curve resolution, J. Phys. Chem. B 113 (2009) 1805–1809.
[25] P.N. Perera, K.R. Fega, C. Lawrence, E.J. Sundstrom, J. Tomlinson-Phillips, D. Ben-Amotz, Observation of water dangling OH bonds around dissolved nonpolar groups, Proc. Natl. Acad. Sci. U. S. A. 106 (2009) 12230–12234.
[26] G. Niehues, M. Heyden, D.A. Schmidt, M. Havenith, Exploring hydrophobicity by THz absorption spectroscopy of solvated amino acids, Faraday Discuss. 49 (2011) 193–207.
[27] F. Bohm, G. Schwaab, M. Havenith, Mapping hydration water around alcohol chains by THz calorimetry, Angew. Chem., Int. Ed. 56 (2017) 9981–9985.
[28] S. Ebbinghaus, S.J. Kim, M. Heyden, X. Yu, U. Heugen, M. Gruebele, D.M. Leitner, M. Havenith, An extended dynamical hydration shell around proteins, Proc. Natl. Acad. Sci. U. S. A. 104 (2007) 20749–20752.
[29] F. Novelli, S.O. Pour, J. Tollerud, A. Roozbeh, D.R.T. Appadoo, E.W. Blanch, J.A. Davis, Time-domain THz spectroscopy reveals coupled protein-hydration dielectric response in solutions of native and fibrils of human lysozyme, J. Phys. Chem. B 121 (2017) 4810–4816.
[30] K.R. Fega, D.S. Wilcox, D. Ben-Amotz, Application of Raman multivariate curve resolution to solvation-shell spectroscopy, Appl. Spectrosc. 66 (2012) 282–288.
[31] K.J. Tielrooij, N. Garcia-Araez, M. Bonn, H.J. Bakker, Cooperativity in ion hydration, Science 328 (2010) 1006–1009.
[32] E.E. Fenn, D.B. Wong, C.H. Giammanco, M.D. Fayer, Dynamics of water at the interface in reverse micelles: measurements of spectral diffusion with two-dimensional infrared vibrational echoes, J. Phys. Chem. B 115 (2011) 11658–11670.
[33] E.E. Fenn, D.B. Wong, M.D. Fayer, Water dynamics at neutral and ionic interfaces, Proc. Natl. Acad. Sci. U. S. A. 106 (2009) 15243–15248.
[34] D. Laage, J.T. Hynes, A molecular jump mechanism of water reorientation, Science 311 (2006) 832–835.
[35] A.C. Fogarty, D. Laage, Water dynamics in protein hydration shells: the molecular origins of the dynamical perturbation, J. Phys. Chem. B 118 (2014) 7715–7729.
[36] Y.Z. Qin, L.Y. Zhang, L.J. Wang, D.P. Zhong, Observation of the global dynamic collectivity of a hydration shell around apomyoglobin, J. Phys. Chem. Lett. 8 (2017) 1124–1131.
[37] T. Li, A.A. Hassanali, Y.T. Kao, D. Zhong, S.J. Singer, Hydration dynamics and time scales of coupled water-protein fluctuations, J. Am. Chem. Soc. 129 (2007) 3376–3382.
[38] Y.Z. Qin, L.J. Wang, D.P. Zhong, Dynamics and mechanism of ultrafast water-protein interactions, Proc. Natl. Acad. Sci. U. S. A. 113 (2016) 8424–8429.
[39] J.T. King, E.J. Arthur, C.L. Brooks, K.J. Kubarych, Crowding induced collective hydration of biological macromolecules over extended distances, J. Am. Chem. Soc. 136 (2014) 188–194.
[40] F. Sterpone, G. Stirnemann, D. Laage, Magnitude and molecular origin of water slowdown next to a protein, J. Am. Chem. Soc. 134 (2012) 4116–4119.
[41] D. Laage, G. Stirnemann, J.T. Hynes, Why water reorientation slows without iceberg formation around hydrophobic solutes, J. Phys. Chem. B 113 (2009) 2428–2435.
[42] J. Han, M.J.M. Mazack, P. Zhang, D.G. Truhlar, J.L. Gao, Quantum mechanical force field for water with explicit electronic polarization, J. Chem. Phys. 139 (2013) 054503.
[43] G.A. Cisneros, K.T. Wikfeldt, L. Ojamae, J.B. Lu, Y. Xu, H. Torabifard, A.P. Bartok, G. Csanyi, V. Molinero, F. Paesani, Modeling molecular interactions in water: from pairwise to many body potential energy functions, Chem. Rev. 116 (2016) 7501–7528.
[44] Z.H. Ma, Y.L. Zhang, M.E. Tuckerman, Ab initio molecular dynamics study of water at constant pressure using converged basis sets and empirical dispersion corrections, J. Chem. Phys. 137 (2012) 044506.
[45] P. Hamm, G.S. Fanourgakis, S.S. Xantheas, A surprisingly simple correlation between the classical and quantum structural networks in liquid water, J. Chem. Phys. 147 (2017) 064506.
[46] K.A.T. Silverstein, A.D.J. Haymet, K.A. Dill, A simple model of water and the hydrophobic effect, J. Am. Chem. Soc. 120 (1998) 3166–3175.
[47] T. Urbic, V. Vlachy, K.A. Dill, Confined water: a Mercedes-Benz model study, J. Phys. Chem. B 110 (2006) 4963–4970.
[48] H.F. Xu, K.A. Dill, Water's hydrogen bonds in the hydrophobic effect: a simple model, J. Phys. Chem. B 109 (2005) 23611–23617.
[49] R.E. Skyner, J.L. McDonagh, C.R. Groom, T. van Mourik, J.B.O. Mitchell, A review of methods for the calculation of solution free energies and the modelling of systems in solution, Phys. Chem. Chem. Phys. 17 (2015) 6174–6191.
[50] J.B. Lu, Y.Q. Qiu, R. Baron, V. Molinero, Coarse-graining of TIP4P/2005, TIP4P-Ew, SPC/E, and TIP3P to monatomic anisotropic water models using relative entropy minimization, J. Chem. Theory Comput. 10 (2014) 4104–4120.
[51] E. Stoll, K. Binder, T. Schneider, Monte-Carlo investigation of dynamic critical phenomena in 2-dimensional kinetic ising-model, Phys. Rev. B 8 (1973) 3266–3289.
[52] A.B. Bortz, M.H. Kalos, J.L. Lebowitz, New algorithm for Monte-Carlo simulation of ising spin systems, J. Comput. Phys. 17 (1975) 10–18.
[53] K.A. Fichthorn, W.H. Weinberg, Theoretical foundations of dynamic Monte-Carlo simulations, J. Chem. Phys. 95 (1991) 1090–1096.
[54] A. Chatterjee, D.G. Vlachos, An overview of spatial microscopic and accelerated kinetic Monte Carlo methods, J. Comput.-Aided Mater. Des. 14 (2007) 253–308.
[55] S.A. Serebrinsky, Physical time scale in kinetic Monte Carlo simulations of continuous-time Markov chains, Phys. Rev. E 83 (2011) 037701.
[56] H.S. Lee, M.E. Tuckerman, Dynamical properties of liquid water from ab initio molecular dynamics performed in the complete basis set limit, J. Chem. Phys. 126 (2007) 164501.
[57] W.D. Moebs, E.A. Haglund, Simple Monte-Carlo method for teaching chemical kinetics, J. Chem. Educ. 53 (1976) 506–507.
[58] N. Smolin, A. Oleinikova, I. Brovchenko, A. Geiger, R. Winter, Properties of spanning water networks at protein surfaces, J. Phys. Chem. B 109 (2005) 10995–11005.
[59] O. Rahaman, M. Kalimeri, M. Katava, A. Paciaroni, F. Sterpone, Configurational disorder of water hydrogen-bond network at the protein dynamical transition, J. Phys. Chem. B 121 (2017) 6792–6798.
[60] V.K.S. Shante, S. Kirkpatrick, Introduction to percolation theory, Adv. Phys. 20 (1971) 325–357.
[61] M.E.J. Newman, The structure and function of complex networks, SIAM Rev. 45 (2003) 167–256.

[62] R. Albert, A.L. Barabasi, Statistical mechanics of complex networks, Rev. Mod. Phys. 74 (2002) 47–97.
[63] A. Oleinikova, I. Brovchenko, N. Smolin, A. Krukau, A. Geiger, R. Winter, Percolation transition of hydration water: from planar hydrophilic surfaces to proteins, Phys. Rev. Lett. 95 (2005) 247802.
[64] A. Oleinikova, N. Smolin, I. Brovchenko, A. Geiger, R. Winter, Formation of spanning water networks on protein surfaces via 2D percolation transition, J. Phys. Chem. B 109 (2005) 1988–1998.
[65] E. Xi, V. Venkateshwaran, L. Li, N. Rego, A.J. Patel, S. Garde, Hydrophobicity of proteins and nanostructured solutes is governed by topographical and chemical context, Proc. Natl. Acad. Sci. U. S. A. 114 (2017) 13345–13350.
[66] R. Barnes, S. Sun, Y. Fichou, F.W. Dahlquist, M. Heyden, S.I. Han, Spatially heterogeneous surface water diffusivity around structured protein surfaces at equilibrium, J. Am. Chem. Soc. 139 (2017) 17890–17901.
[67] E.J. Arthur, J.T. King, K.J. Kubarych, C.L. Brooks, Heterogeneous preferential solvation of water and trifluoroethanol in homologous lysozymes, J. Phys. Chem. B 118 (2014) 8118–8127.
[68] M. Heyden, D.J. Tobias, Spatial dependence of protein-water collective hydrogen-bond dynamics, Phys. Rev. Lett. 111 (2013) 218101.
[69] S. Perticaroli, G. Ehlers, C.B. Stanley, E. Mamontov, H. O'Neill, Q. Zhang, X.L. Cheng, D.A.A. Myles, J. Katsaras, J.D. Nickels, Description of hydration water in protein (green fluorescent protein) solution, J. Am. Chem. Soc. 139 (2017) 1098–1105.
[70] G.R. Medders, V. Babin, F. Paesani, Development of a "First-Principles" water potential with flexible monomers. III. Liquid phase properties, J. Chem. Theory Comput. 10 (2014) 2906–2910.
[71] G.R. Medders, A.W. Gotz, M.A. Morales, P. Bajaj, F. Paesani, On the representation of many-body interactions in water, J. Chem. Phys. 143 (2015) 104102.
[72] G.R. Medders, F. Paesani, Infrared and Raman spectroscopy of liquid water through "First-Principles" many-body molecular dynamics, J. Chem. Theory Comput. 11 (2015) 1145–1154.
[73] M. Riera, E. Lambros, T.T. Nguyen, A.W. Gotz, F. Paesani, Low-order many-body interactions determine the local structure of liquid water, Chem. Sci. 10 (2019) 8211–8218, https://doi.org/10.1039/c1039sc03291f.